ORIGINAL ARTICLE

Fenretinide Treatment Prevents Diet-Induced Obesity in Association With Major Alterations in Retinoid Homeostatic Gene Expression in Adipose, Liver, and Hypothalamus

George D. McIlroy, Mirela Delibegovic, Carl Owen, Patrick N. Stoney, Kirsty D. Shearer, Peter J. McCaffery, and Nimesh Mody

The synthetic retinoid, Fenretinide (FEN), inhibits obesity and insulin resistance in mice and is in early clinical trials for treatment of insulin resistance in obese humans. We aimed to determine whether alterations in retinoic acid (RA)-responsive genes contribute to the beneficial effects of FEN. We examined the effect of FEN on 3T3-L1 adipocyte differentiation and alterations in gene expression in C57Bl/6 and retinaldehyde dehydrogenase (*RALDH*) 1 knockout (KO) mice fed a high-fat (HF) diet. FEN completely inhibited adipocyte differentiation by blocking CCAAT/enhancer-binding protein (*C/EBP*) α/peroxisome proliferator–activated receptor (*PPAR*) γ−mediated induction of downstream genes and upregulating RA-responsive genes like cellular retinol-binding protein-1. In mice fed an HF diet, RA-responsive genes were markedly increased in adipose, liver, and hypothalamus, with short-term and long-term FEN treatment. In adipose, FEN inhibited the downregulation of *PPARγ* and improved insulin sensitivity and the levels of *adiponectin*, resistin, and serum RBP (RBP4). FEN inhibited hyperleptinemia in vivo and *leptin* expression in adipocytes. Surprisingly, hypothalamic neuropeptide Y expression was completely suppressed, suggesting a central effect of FEN to normalize hyperglycemia. Moreover, FEN induced RA-responsive genes in *RALDH1* KO mice, demonstrating that FEN can augment RA signaling when RA synthesis is impaired. We show that FEN-mediated beneficial effects are through alterations in retinoid homeostasis genes, and these are strong candidates as therapeutic targets for the treatment of obesity and insulin resistance. *Diabetes* 62:825–836, 2013

More than one-third of United States adults are obese and at risk for development of type 2 diabetes and a host of other metabolic disorders, including dyslipidemia and cardiovascular disease. Despite the development and clinical use of many antidiabetes drugs, they are limited by adverse effects such as fluid retention, weight gain, congestive heart failure, liver toxicity, and the potential for carcinogenesis (1). Therefore, alternative therapies for the treatment of obesity and type 2 diabetes are needed.

The synthetic retinoid, Fenretinide [*N*-(4-hydroxyphenyl) retinamide] (FEN) prevents obesity and insulin resistance

in mice fed a high-fat (HF) diet (2,3). In addition, FEN lowers serum retinol–binding protein (gene name *RBP4*) levels in rodents and humans by disrupting the ternary complex of retinol-RBP4-transthyretin and thereby by promoting renal clearance of RBP4 (4,5). However, the antiobesity action of FEN appears to be independent of its ability to lower circulating levels of this protein because FEN reduces obesity development in mice lacking *RBP4* and does not appear to alter food intake or energy expenditure (3). Currently, FEN is undergoing a phase II trial for treatment of insulin resistance in obese humans with hepatic steatosis (6). Thus, the mechanisms by which FEN can prevent obesity and insulin resistance are of great interest. FEN was originally developed as a chemotherapeutic agent (7), and then was found to attenuate cancer cell growth by mechanisms such as apoptosis and reactive oxygen species generation. However, these effects appear to vary in different cells (8). FEN is now the most widely studied retinoid in clinical trials of breast cancer chemoprevention because of its selective accumulation in breast tissue and its favorable toxicological profile (9,10). One mild and reversible side effect is a reduction in circulating retinol levels and deficits in dark adaptation attributable to lowering of circulating RBP4 levels (4,5,11).

Retinoid homeostasis is tightly regulated by a complex system of enzymes and carriers that can promote the storage of retinol in the form of retinyl esters (RBP4, cellular RBP1, CRBP1, and lecithin:retinol acyltransferase); metabolism to retinoic acid (RA) and signaling through its receptors (retinaldehyde dehydrogenase [RALDH1], cellular RA-binding protein, CRABP, and RA receptors [RARs]); and degradation via cytochrome P450-type enzymes (CYP26A1) (12). It has long been known that RA potently blocks adipogenesis when introduced at early stages of differentiation (13–15). More recently, the importance of retinoid homeostasis in whole-body energy balance and glucose homeostasis has been highlighted in genetic knockout (KO) studies of *RALDH1* (lean phenotype), *CRBP1*, and *CRABP1* (obese phenotype) (16–18). Because initial mouse studies indicated that FEN could be a promising therapeutic agent to treat or prevent obesity, and because insulin resistance, glucose intolerance, and human cancer trials have demonstrated few side effects, we sought to further investigate the mechanisms by which FEN inhibits adiposity and alters glucose and lipid homeostasis. We aimed to determine whether FEN inhibits adipocyte differentiation and alters adipose and hepatic gene expression, and whether alterations in retinoid

homeostasis could contribute to the mechanism of FEN-induced leanness in the setting of diet-induced obesity.

RESEARCH DESIGN AND METHODS

Cell culture. The 3T3-L1 preadipocytes (ZenBio) were cultured in Dulbecco's modified Eagle's medium (DMEM) with 10% bovine calf serum (16170; Gibco) and 1% pyruvate (growth media). Differentiation was induced 2 days postconfluency with DMEM containing 10% fetal bovine serum (A15-104; PAA), 1% pyruvate, 1% penicillin/streptomycin, 1 μmol/L dexamethasone, 0.5 mmol/L 3-isobutyl-1-methylxanthine, and 10 μg/mL insulin (MDI media). MDI media were removed after 48 h and were replaced every 2 days with MDI media without 3-isobutyl-1-methylxanthine and dexamethasone. FEN, RA, and rosiglitazone (ROSI) were dissolved in DMSO and added as indicated (see figure legends). FEN was a generous gift from U. Thurneer (Cilag AG, Switzerland). Cells were tested for viability using Resazurin assays (R&D Systems).

Animals. Male C57BL/6 wild-type mice were from Charles River (Edinburgh, UK). Mice were group-housed (four per box) for gene expression studies or individually housed for food intake and calorimetry, were exposed to 12-h/12-h light–dark, and had ad libitum access to food and water. Three-month-old mice were randomized by body weight and were administered a 45% HF diet (D12450B; Research Diets, New Brunswick, NJ), HF-containing 0.04% wt/wt FEN (Research Diets), or chow diet (801722 CRM(P); Special Diets Service) for the duration of the studies. FEN HF mice received FEN ~30 mg/kg per day. Six-week-old mice were used for the short-term diet study. RALDH1 KO mice were generously provided by G. Duester (19); RBP4 KO mice were provided by L. Quadro (20). Mice were killed at the end of each experiment by cardiac exsanguination under CO_2-induced anesthesia or cervical dislocation. Hypothalamus was precisely dissected from fresh brains on an ice-cold platform following anatomical landmarks. All tissues were rapidly dissected, frozen in liquid nitrogen, and stored at −80°C. Animal procedures were approved by University of Aberdeen Ethics Review Board and performed under license (PPL60/3951) approved by the UK Home Office.

Metabolic studies. Body composition was measured by dual-energy X-ray absorptiometry (Lunar PIXIMUS-Densitometer; GE Medical Systems). Metabolic rate (energy expenditure) was measured by indirect, open-circuit calorimetry (CLAMS; Columbus Instruments) during 4–6 weeks of diet. All mice were acclimatized to monitoring cages for 3 h before measurements of O_2 consumption. Food intake was measured every 3 days from initiation of diet for 4 weeks, during weeks 10–12 during long-term diet treatment, and before and during short-term treatment. Serum insulin, leptin, resistin, tumor necrosis factor-α, and interleukin-6 were measured using Milliplex Adipokine Panel (MADPK-71K; Millipore) on the Luminex platform at 20 weeks of diet treatment. On all other occasions, serum leptin was measured by ELISA (Crystal Chem). Serum glucose was measured by glucose oxidase assay (TR15103; Thermo) after collection of blood from tail vein of live mice.

Lipogenesis assay. The assay was performed as described previously (21). Briefly, mice fed ad libitum were killed by cervical dislocation at 18 weeks of diet and perigonadal adipose was dissected. Adipocytes were isolated, resuspended (2% packed cell volume), and incubated with D-[6-^{3}H] glucose and insulin. Triplicate assays were stopped with scintillation liquid and ^{3}H lipid was measured.

Gene expression analysis. Total RNA was isolated from frozen tissue or 3T3-L1 monolayers using peqGOLD TriFast (Peqlab). Specifically for adipose, TriFast homogenates were centrifuged and lipid layer was removed before phase separation. cDNA was synthesized using Bioscript cDNASynthesis Kit (Bioline), 1 μg RNA, and oligo (dT) 18 primers and random hexamer primers. Quantitative PCR was performed using GoTaq qPCR Master Mix (Promega) and gene-specific primers on the LightCycler-480 (Roche). Relative mRNA levels were calculated using the Pfaffl method (22) normalized to hypoxanthine-guanine phosphoribosyltransferase or 18S.

Immunoblotting. Frozen tissue lysates were prepared in RIPA buffer and SDS-PAGE was performed and transferred to nitrocellulose (21). The following antibodies were used: total insulin receptor sc-711; total Akt/protein kinase B (PKB) sc-8312 (Santa Cruz); RBP4 (Dako); phospho-Akt/PKB 9271; phospho-S6 4858; phospho-ERK1/2 4376; adipose triglyceride lipase (ATGL) 2138 and HSL 4107 (Cell Signaling); and phospho-insulin receptor 44804G (Invitrogen). Proteins were visualized using enhanced chemiluminescence and were quantified with Image J software or Fusion imaging system and Bio-1D software (Peqlab).

Statistical analysis. Data are presented as means ± SEM and were compared using one-way ANOVA with post hoc tests or Student t test (when indicated in figure legends).

RESULTS

Fenretinide inhibits 3T3-L1 differentiation. Because RA has been shown to inhibit adipocyte differentiation, we examined the effect of FEN on adipocyte differentiation in 3T3-L1 cells. The 1 μmol/L FEN potently inhibited 3T3-L1 differentiation (Fig. 1A). Similar inhibition was obtained with RA, whereas the peroxisome proliferator–activated receptor (PPAR) γ activator ROSI, a potent inducer of the adipogenic program, was used to stimulate the rate of differentiation. Up to five-fold higher FEN did not affect cell viability (Supplementary Fig. 1). Terminal markers of adipogenesis aP2, CD36, adiponectin, and lipoprotein lipase LPL were almost completely inhibited by FEN or RA (Fig. 1B). GLUT4 mRNA was highly expressed in differentiated cells but was not detected in undifferentiated control (−VE CONT), RA, or FEN cells (data not shown). Similar results were obtained with the upstream intermediate markers PPARγ and C/EBPα (Fig. 1C). Expression of C/EBPβ mRNA, which normally increases transiently during early phases of adipogenesis, was not affected by FEN or RA (Fig. 1C).

Because FEN is a synthetic retinoid, we tested its effects on retinoid-signaling genes (Fig. 1D and 1E). RARα was transiently upregulated with differentiation, and this was prevented by RA only. RARγ levels were downregulated during differentiation, and this was prevented by RA or FEN and expression levels induced above those of −VE CONT cells. RARβ was not expressed in these cells. RA signaling can be further regulated by several proteins controlling retinoid metabolism that are themselves regulated by RA signaling via RA response elements (RAREs) in their promoters. CRBP1, RALDH1, and CRABP2 all were upregulated with RA or FEN (Fig. 1E). The major degradation enzyme for RA, CYP26A1, was markedly repressed by induction of differentiation, and this trended to be inhibited by FEN or RA. Strikingly, all the retinoid metabolism genes examined were coordinately repressed with ROSI treatment (Fig. 1D and 1E).

Fenretinide inhibits lipid accumulation in fully differentiated 3T3-L1 adipocytes. Next, we tested if FEN could reduce lipid accumulation in fully differentiated 3T3-L1 cells (Fig. 2), because FEN has been shown to inhibit adiposity and adipocyte lipid content in vivo (3). As expected, RA did not affect lipid accumulation in fully differentiated 3T3-L1 cells (15); however, FEN treatment significantly reduced lipid content by 26% (Fig. 2A). The mechanism of this reduction may involve a coordinate reduction in the expression levels of adipocyte genes fatty acid synthase (FAS), LPL, hormone-sensitive lipase (HSL), ATGL, leptin, and RBP4 to levels lower than in vehicle (VEH) and/or RA-treated adipocytes (Fig. 2B and C). FEN significantly induced CRBP1 and RALDH1, and it induced small increases in RARα and RARγ, but it did not affect the expression of other retinoid genes measured (Fig. 2C). To test whether FEN-treated cells were more insulin-sensitive, cells were stimulated with insulin and Akt/PKB phosphorylation was analyzed. Akt/PKB phosphorylation was increased 3.5-fold in FEN-treated adipocytes, indicating improved insulin sensitivity (Fig. 2D).

Fenretinide improves adipokine levels in mice with HF-induced obesity. Next, we investigated whether FEN treatment would induce similar alterations in vivo. In C57Bl/6 mice, FEN treatment prevented body weight gain over the course of 20 weeks of HF feeding (Fig. 3A), inhibited adiposity (Fig. 3B), and completely normalized
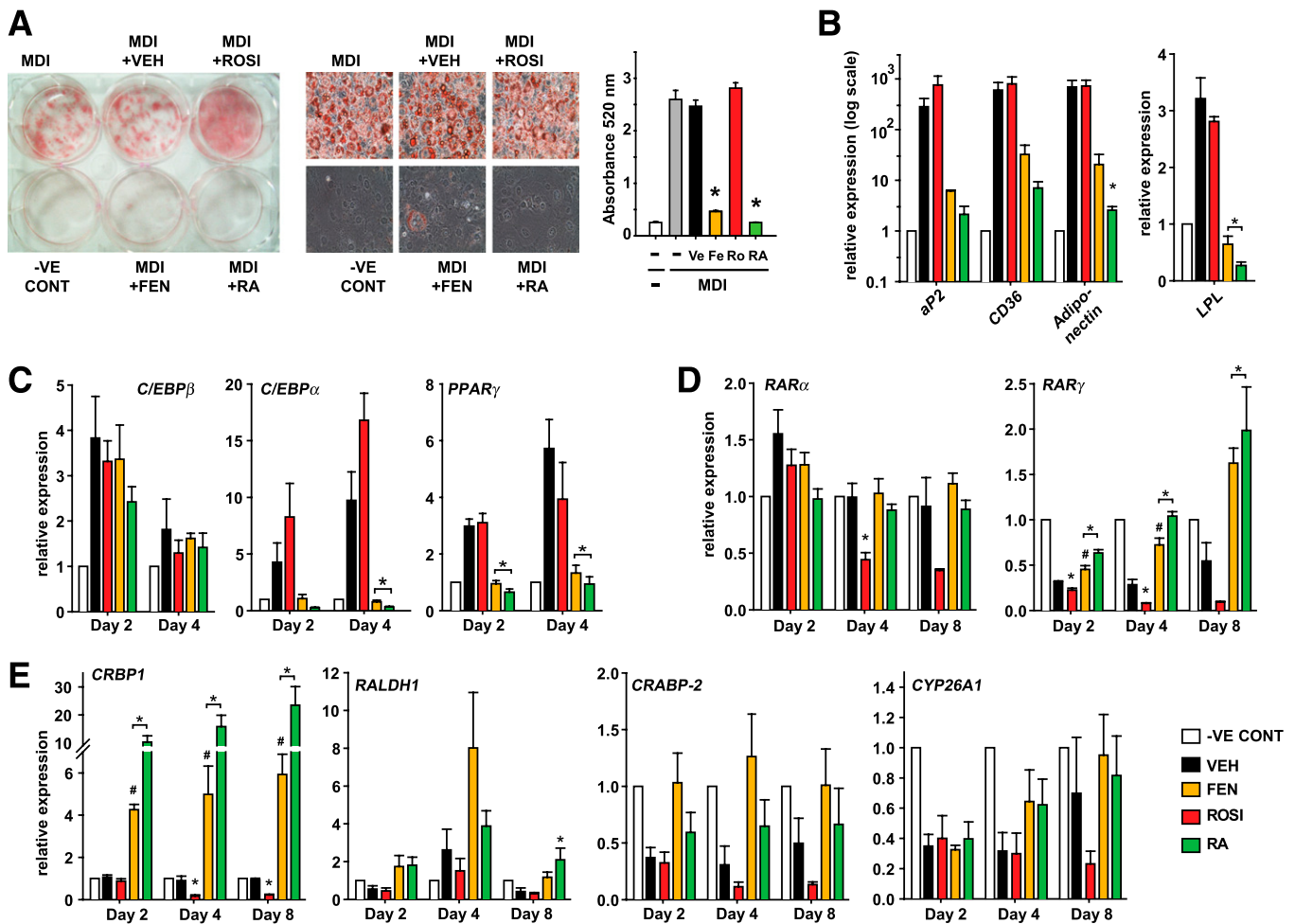
FIG. 1. FEN inhibits 3T3-L1 preadipocyte differentiation and upregulates retinoid responsive genes. *A*: Oil-red-O staining and lipid quantification of 3T3-L1 adipocytes differentiated for 8 days with MDI media and indicated compounds (FEN, RA, and ROSI at 1 μmol/L or DMSO as vehicle [VEH]) added at day 0. RA was used as a known inhibitor and ROSI was used as a promoter of differentiation. Middle panels show 40× images of representative cell morphology and staining from six-well plate (left panel). Total lipid was quantified by eluting the stain and measuring absorbance at 520 nm (right panel). Significance ($P < 0.05$ by one-way ANOVA followed by Tukey post hoc test or *t* test if indicated) is shown by *ROSI, FEN, or RA compared with VEH or #FEN compared with RA. *B*: Gene expression of terminal adipocyte markers at day 8 of 3T3-L1 differentiation observed in cell treatments shown in (*A*: undifferentiated control [−VE CONT], clear bar; VEH, black bar; ROSI, red bar; FEN, orange bar; RA, green bar). *aP2*, *CD36*, and *adiponectin* FEN compared with VEH trended to be significantly different by *t* test ($P = 0.097$, 0.086, and 0.051, respectively). *C*: Early gene marker profile of key transcription factors involved in the induction of adipogenesis. Cells were treated with MDI media and the indicated compounds as in (*A*). Relative expression of genes was measured at the indicated time points. *D* and *E*: Gene expression profile of retinoid metabolism–related genes. Time points indicate day of differentiation from cell treatments shown in (*A*). The *t* test was used to calculate significant difference for *RARγ* on day 2 and 4, ROSI compared with VEH and on day 8, FEN vs. VEH and for *CRBP1* on day 2, 4, and 8, FEN compared with VEH and on day 4 and 8 ROSI vs. VEH. Otherwise significance was calculated by ANOVA. Gene expression was analyzed by quantitative PCR analysis. MDI values were removed because no significant differences were observed between MDI ± VEH in all cases. Data represents mean ± SEM of three separate experiments (performed on different days and different passage cells). (A high-quality digital representation of this figure is available in the online issue.)

hyperglycemia (Table 1). FEN did not affect lean mass (not shown). White adipose tissue (WAT) dissected from FEN mice and the lipid layer after aqueous buffer homogenization were yellow instead of the normal white or pink (Fig. 3*C*), suggesting accumulation of FEN (a retinoid with peak UV absorbance at 300–400 nm). Similarly, clinical trials for breast cancer chemoprevention have shown FEN to selectively accumulate in breast, a characteristically fatty tissue (23,24). Thus, we tested whether FEN was acting directly on WAT. As expected, serum leptin levels were reduced (Table 1). Serum RBP4 levels are reduced with FEN treatment (2,5); however, it is not known if FEN affects tissue RBP4 protein levels in vivo. We found that adipose RBP4 protein levels were decreased 40% with FEN compared with HF-fed and chow-fed mice (Table 1). However, hepatic RBP4 protein levels were increased

compared with HF-fed mice (Table 1). Elevated levels of serum resistin with HF feeding also were attenuated with FEN treatment (Table 1). Circulating levels and adipose mRNA levels of *adiponectin* are reduced in obesity and insulin resistance. We found adipose *adiponectin* mRNA levels were partially normalized, up 63% with FEN treatment (Table 1). Thus, multiple adipose-secreted factors that are altered and implicated in the pathology of obesity and insulin resistance are modulated toward normality by FEN treatment.

Fenretinide partially normalizes adipose insulin sensitivity in mice fed HF diet. In association with normalized glycemia, serum insulin levels also were markedly lower in FEN-treated mice compared with HF (Table 1). Insulin receptor (IR) protein levels are downregulated in obesity and insulin resistance, inversely
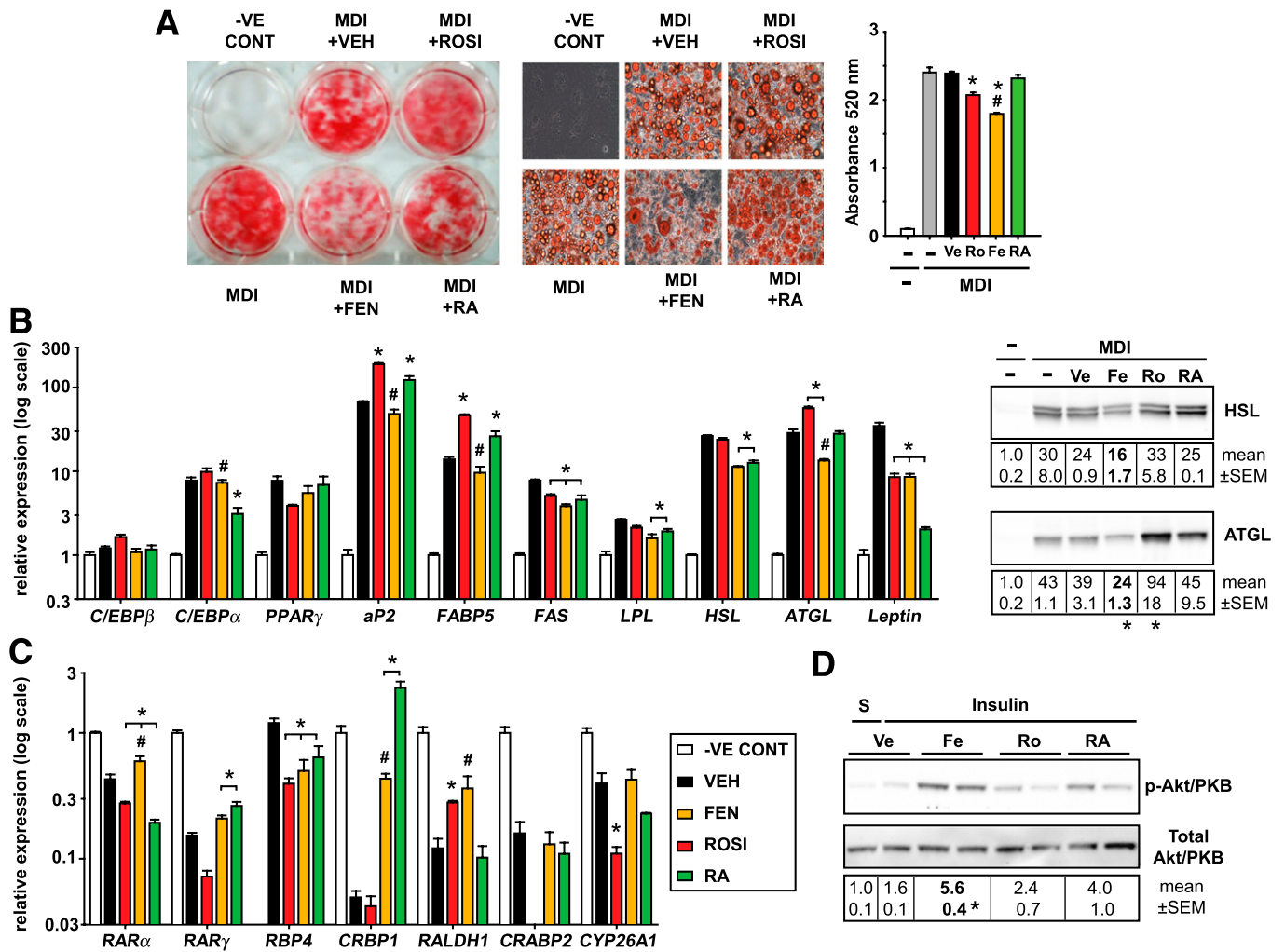
FIG. 2. Identification of divergent effects of FEN in fully differentiated adipocytes. *A*: Differentiated 3T3-L1 adipocytes were used to determine if FEN could reduce lipid content of mature adipocyte cells. 3T3-L1 cultures were differentiated with MDI alone for 8 days and then were subjected to the indicated treatments for an additional 8 days (FEN, RA, and ROSI at 1 µmol/L). Oil-red-O staining and lipid accumulation quantification of 3T3-L1 adipocytes revealed FEN significantly reduced triglyceride levels, unlike RA, which did not significantly change. MDI plus VEH had equivalent DMSO added as treated cells. Middle panels show 40× images of representative cell morphology/staining from six-well plate (left panel). Total lipid was quantified by eluting the stain and measuring absorbance at 520 nm (right panel). All graphs represent mean ± SEM of three separate experiments (performed on different plates of cells). Significance ($P < 0.05$ by one-way ANOVA followed by Tukey post hoc test or *t* test if indicated) is shown for *ROSI, FEN, or RA compared with vehicle (VEH) or for #FEN vs. RA. *B*: Relative expression levels of adipocyte genes observed from cultures described in (*A*) (quantitative PCR analysis, left panel). Immunoblots of HSL and ATGL protein levels (right panel). The *t* test was used to calculate significant difference for ATGL FEN or ROSI compared with VEH. HSL FEN vs. VEH trended to be significantly different by *t* test ($P = 0.06$). $N = 2$ different plates of cells. Otherwise significance was calculated by ANOVA. *C*: Retinoid metabolism gene expression levels observed in 3T3-L1 cultures shown in (*A*). The *t* test was used to calculate significant difference for *RARγ* FEN or RA vs. VEH, for *CRBP1* FEN vs. VEH, *RALDH1* ROSI or FEN vs. VEH, and *CYP26A1* ROSI vs. VEH. Otherwise significance was calculated by ANOVA. *D*: Differentiated 3T3-L1 adipocytes were stimulated with 10 nmol/L insulin (for 15 min after overnight serum-free media) or saline (S) to determine if Fenretinide could increase insulin sensitivity of mature adipocyte cells. Phosphorylation of Akt/PKB at Ser473 and total Akt/PKB protein expression were determined by immunoblotting and the signal quantified. $n = 2$ different plates of cells. (A high-quality digital representation of this figure is available in the online issue.)

correlating with circulating insulin levels (25,26). We found adipose IR protein levels to be downregulated in HF (Fig. 3*D*, left panel), inversely correlating with obesity (not shown) and serum insulin levels (Fig. 3*D*, right panel), and this decrease was attenuated with FEN treatment. Thus, we measured insulin-stimulated lipogenesis in WAT ex vivo as an indicator of WAT insulin sensitivity. Basal lipogenesis in WAT was not altered in HF or FEN HF mice; however, insulin-stimulated lipogenesis was markedly decreased in HF mice and normalized ~40% in FEN HF mice (Fig. 3*E*). Moreover, in mice injected with a bolus of insulin, adipose tissue phosphorylation of Akt/PKB trended to be higher, whereas phosphorylation of p70 S6 kinase

substrate S6 and of ERK1/2 were significantly decreased (Fig. 3*F*). S6 kinase is implicated in negative feedback inhibition of insulin signaling, and mice lacking adipose mTORC1–S6 kinase signaling or whole-body ERK1 are lean. Muscle insulin signaling was unaltered (Supplementary Fig. 2). Together, these findings indicate that improvements in adipose insulin signaling are part of the mechanism by which FEN exerts its beneficial action.

FEN alters adipose and hepatic gene expression. Next, we examined other metabolic genes in WAT that may be altered by HF feeding, obesity, and insulin resistance. We found *PPARγ* and *C/EBPα* were decreased ~50% with HF diet, whereas the decrease in FEN was
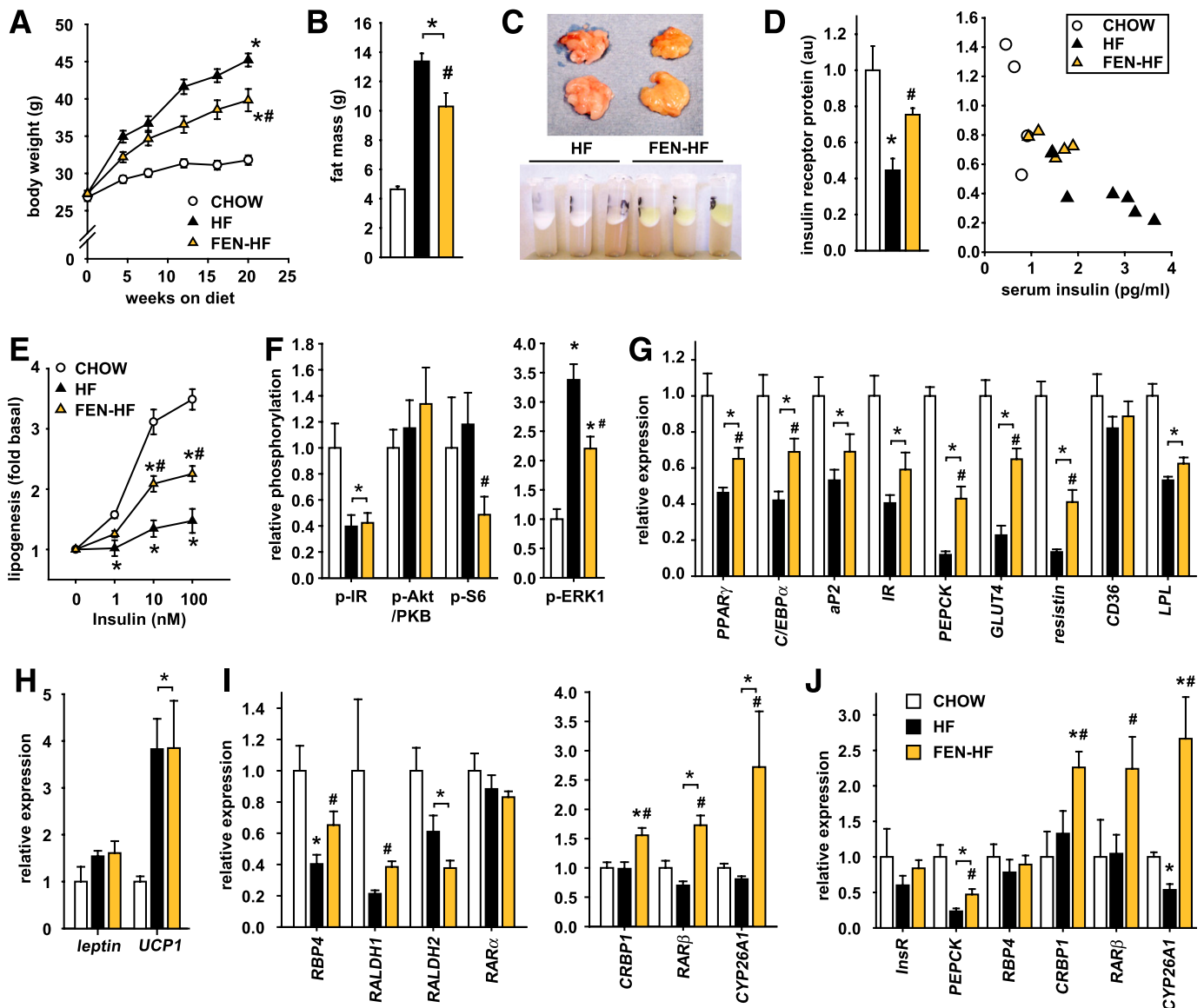
FIG. 3. FEN accumulates in adipose tissue and alters adipose gene expression in HF diet–fed mice. *A*: Body weight curves of male C57BL/6 mice fed chow (clear circles, *n* = 16), HF diet (HF; black triangles, *n* = 24), or HF plus 0.04% wt/wt FEN (FEN-HF; gold triangles, *n* = 16) from 3 months of age, significance was calculated by one-way ANOVA Bonferroni post hoc test. *P < 0.05 vs. chow; #P < 0.05 vs. HF (except at 8 weeks of diet). *B*: Body fat content at 12 weeks on diet (chow, clear bar; HF, black bar; or FEN-HF, gold bar). *C*: Yellow coloration of abdominal adipose tissue in FEN-HF mice dissected after 20 weeks of diet treatment (top panel) and fat layer of adipose RIPA lysates after centrifugation (bottom panel). *D*: Insulin receptor protein levels in perigonadal adipose quantified after immunoblot (left panel: chow, clear bar; HF, black bar; or FEN-HF, gold bar). Negative correlation of IR protein levels in perigonadal adipose with serum insulin levels at 20 weeks of diet (right panel: chow, clear circles; HF, black triangles; or FEN-HF, gold triangles). *E*: Insulin-stimulated adipose lipogenesis measured ex vivo in perigonadal adipose. Chow (clear circles), HF (black triangles), or FEN-HF (gold triangles). *F*: Insulin-stimulated adipose signaling in vivo. Mice were fasted overnight, injected intraperitoneally with 10 mU/g insulin or saline for 10 min and tissues dissected. Phosphorylation of IR, Akt/PKB, S6, and ERK1 were determined by immunoblotting and signal quantified (chow, clear bar; HF, black bar; or FEN-HF, gold bar; *n* = 4–6 mice). The *t* test was used to calculate significant difference for p-S6 FEN vs. HF. Otherwise significance was calculated by ANOVA. *G–J*: Relative expression levels in perigonadal WAT of metabolic (*G*), energy expenditure (*H*), and retinoid homeostasis (*I*) genes, and in subcutaneous WAT (*J*), chow (clear bars), HF (black bars), or FEN-HF (gold bars). Molecular analysis was performed from six to eight mice per dietary group. The *t* test was used to calculate significant difference for perigonadal WAT *PPARγ, C/EBPα, RBP4,* and *RALDH1* for FEN-HF vs. HF, *aP2* FEN vs. chow and *RARβ* HF vs. chow, subcutaneous WAT *PEPCK* all comparisons, *RARβ* FEN vs. HF, and *CYP26A1* chow vs. HF. Otherwise significance was calculated by ANOVA. (A high-quality digital representation of this figure is available in the online issue.)

significantly less (~30%). Similar gene expression changes were observed with *IR, aP2,* and *LPL* (Fig. 3*G*). *GLUT4, PEPCK,* and *resistin* were decreased ~80–90% with HF diet, but were three-fold higher with FEN (Fig. 3*G*). *CD36, leptin,* and *UCP1* mRNA were unaltered with FEN treatment (Fig. 3*G* and *H*). Next, we tested whether FEN could alter expression of retinoid metabolism and signaling genes. Adipose *RBP4* and *RALDH1* mRNA levels were

downregulated with HF diet, and this was attenuated with FEN, similar to *PPARγ* levels (Fig. 3*I*). Strikingly, FEN treatment strongly induced the *CRBP1, RARβ,* and *CYP26A1* in WAT, above and beyond the levels in chow-fed mice (Fig. 3*I*). Similar data were obtained from subcutaneous WAT (Fig. 3*J*). Moreover, we found *CRBP1, RARβ,* and *CYP26A1* were similarly upregulated in the liver of FEN mice, whereas *RBP4* levels were downregulated

TABLE 1
Serum parameters and tissue levels of metabolically important secreted factors

	Chow	HF	FEN-HF
Serum levels			
Glucose (mmol/L)	11.9 ± 0.7	20.9 ± 0.2†	11.6 ± 0.6¶
Insulin (ng/mL)	0.7 ± 0.08	2.8 ± 0.3†	1.6 ± 0.2‡
Leptin (ng/mL)	1.3 ± 0.5	14.0 ± 1.2†	9.27 ± 1.0†‡
Resistin (ng/mL)	2.3 ± 0.4	5.0 ± 0.4†	3.3 ± 0.5‡
Tumor necrosis factor-α (pg/mL)	3.5 ± 0.7	3.2 ± 0.2	3.6 ± 0.4
IL-6 (pg/mL)	47.3 ± 15.1	6.8 ± 1.9	16.0 ± 4.2
Tissue levels (fold-change vs. chow)			
RBP4, adipose protein	1.0 ± 0.05	1.02 ± 0.08	0.62 ± 0.04†¶
RBP4, liver protein	1.0 ± 0.12	0.73 ± 0.06	1.07 ± 0.10‡
Adiponectin, adipose mRNA	1.0 ± 0.17	0.37 ± 0.06†	0.60 ± 0.04*‡

*$P < 0.05$; †$P < 0.001$ for HF or FEN-HF vs. chow; ‡$P < 0.05$ and ¶$P < 0.001$ for FEN vs. HF. Serum glucose was measured at 12 weeks of diet treatment and all other factors at 20 weeks, both after 5-h food removal. Data are presented as mean ± SEM with significance tested using one-way ANOVA. For *adiponectin*, one-way ANOVA was not significant for FEN-HF vs. HF; however, ‡ indicates $P = 0.006$ with a *t* test.

(Table 2). We also found that HF-induced elevations in liver triglycerides were substantially decreased with FEN treatment (Table 2). These findings were linked with increased expression of fatty acid transporter *CD36* with HF diet that was prevented with FEN (Table 2). Overall, these findings suggest that long-term FEN treatment causes partial normalization of altered metabolic gene expression and potent induction of RA signaling in adipose tissue and liver, despite a reduction in circulating retinol levels.

Effect of FEN on energy expenditure, food intake, and hypothalamic gene expression. Despite exhibiting decreased adiposity and serum leptin levels, indirect calorimetry did not show an increase in oxygen consumption as a potential mechanism of FEN action (Fig. 4*A* and *B*). Rather, oxygen consumption per mouse increased linearly

TABLE 2
Liver gene expression and triglyceride levels

	Chow	HF	FEN-HF
Liver triglyceride (mg/g tissue)	15.4 ± 2.0	56.5 ± 5.0†	29.4 ± 5.7#
Metabolic genes			
5-h fasted			
PPARγ	1.0 ± 0.05	0.8 ± 0.08	0.6 ± 0.03*#
CD36	1.0 ± 0.1	2.5 ± 0.26*	1.3 ± 0.21#
LPL	1.0 ± 0.11	0.7 ± 0.23	1.0 ± 0.30
PPARα	1.0 ± 0.06	0.7 ± 0.04*	0.6 ± 0.05*
FAS	*1.0 ± 0.13*	0.8 ± 0.19	0.5 ± 0.05*
Fed ad libitum			
PPARγ	1.0 ± 0.089	1.2 ± 0.12	1.5 ± 0.12*
CD36	1.0 ± 0.08	2.4 ± 0.40*	2.2 ± 0.30*
LPL	1.0 ± 0.07	1.1 ± 0.19	1.1 ± 0.13
PPARα	1.0 ± 0.06	1.3 ± 0.09	1.4 ± 0.11
FAS	*1.0 ± 0.12*	0.4 ± 0.10*	0.3 ± 0.05*
PEPCK	1.0 ± 0.11	0.8 ± 0.14	0.7 ± 0.09
IR	1.0 ± 0.03	0.9 ± 0.05	0.9 ± 0.06
Retinoid genes			
5-h fasted			
RBP4	1.0 ± 0.05	0.9 ± 0.03	0.8 ± 0.04*
CRBP1	1.0 ± 0.23	0.5 ± 0.14	2.3 ± 0.53‡
RALDH1	1.0 ± 0.07	1.1 ± 0.08	0.8 ± 0.03‡
RARβ	1.0 ± 0.06	0.8 ± 0.09	2.4 ± 0.25†¶
CYP26A1	1.0 ± 0.14	0.5 ± 0.07	28.4 ± 1.62†¶
Fed ad libitum			
RBP4	1.0 ± 0.04	0.9 ± 0.05	0.7 ± 0.04†‡
CRBP1	1.0 ± 0.11	0.9 ± 0.21	2.4 ± 0.28†¶
RALDH1	1.0 ± 0.08	1.4 ± 0.16	1.1 ± 0.06
RALDH2	1.0 ± 0.13	1.0 ± 0.15	1.2 ± 0.16
RARα	1.0 ± 0.09	1.2 ± 0.04	1.3 ± 0.09*
RARβ	1.0 ± 0.07	0.8 ± 0.06	2.5 ± 0.16†¶
CYP26A1	1.0 ± 0.16	0.3 ± 0.07	12.7 ± 1.43†¶

*$P < 0.05$, †$P < 0.001$ for HF or FEN-HF vs. chow and ‡$P < 0.05$ and ¶$P < 0.001$ for FEN vs. HF. Data are presented as mean ± SEM with significance tested using one-way ANOVA.

with increased body mass in HF-fed mice (Fig. 4*C*) and, thus, FEN mice had marginally lower oxygen consumption, appropriate for their weight. Food intake was unaltered with FEN treatment (Fig. 4*D*). In brown adipose tissue, there was a clear upregulation of *CRBP1* and a trend for upregulation of *CYP26A1* by FEN; however, *UCP1*, *IR*, *PEPCK*, and *RARβ* mRNAs were the same in HF and FEN HF mice (Fig. 4*E*).

Despite not affecting energy expenditure or food intake, we found that FEN completely suppressed hypothalamic *NPY* gene expression (Fig. 4*F*). In addition, FEN induced hypothalamic *RALDH1*, *RADLH2*, and *RARα* mRNAs, indicating a central affect of FEN treatment.

Effect of short-term FEN treatment on adipose and hepatic gene expression. The large changes in adipose and hepatic gene expression seen in Fig. 3 were associated with long-term FEN treatment (20 weeks), relative leanness, and major improvements in glucose homeostasis. Next, we tested whether long-term FEN treatment was required for these effects. After 1 week of HF diet or FEN and HF diet, both groups gained ~2 g more than mice fed a chow diet; however, there was a trend for decreased body weight with FEN treatment (Fig. 5*A*). This effect was not associated with decreased food intake (Fig. 5*B*). Strikingly, FEN prevented the HF-induced elevation in serum leptin levels (Fig. 5*C*), with a similar trend for *leptin* mRNA in WAT, without an effect on other metabolic genes such as *GLUT4*, *adiponectin*, or *PEPCK* (Fig. 5*D*). In addition, FEN prevented the HF-induced decrease in *CRBP1* mRNA in WAT. Short-term FEN treatment also decreased *RBP4* mRNA and induced an increase in *RARβ* and *CYP26A1* in WAT relative to both HF-fed and chow-fed mice (Fig. 5*D*). HF diet led to a characteristic marked downregulation of hepatic *SCD-1* (Fig. 5*E*) and a 20–30% decrease in adipose *GLUT4* (Fig. 5*D*) mRNA in both HF and FEN HF mice. Hepatic *PEPCK*, a known target of RA signaling, was induced in liver with short-term FEN. No other differences in metabolic genes were observed in liver with short-term FEN; however, *CRBP1*, lecithin: retinol acyltransferase (*LRAT*), *RARβ*, and *CYP26A1* all were markedly induced. In addition, we found that hypothalamic *NPY* mRNA was reduced 29% and 14% with FEN compared with chow diet or HF diet, respectively (Fig. 5*F*). Thus, short-term FEN treatment is sufficient to induce RA signaling in adipose tissue, liver, and hypothalamus.

Gene expression alterations in RALDH1 KO and RBP4 KO mice. Mice lacking the enzyme RALDH1 are compromised in their ability to make RA (19) and have been shown to be resistant to obesity and insulin resistance (16). We examined whether changes in gene expression induced by FEN treatment in normal mice are similarly altered in mice lacking *RALDH1*. We confirmed that *RALDH1* KO mice are resistant to HF-induced obesity (Fig. 6*A*). In adipose tissue, key metabolic genes that are downregulated in obesity were approximately two-fold higher in *RALDH1* KO mice. Moreover, *RBP4*, *CRBP1*, and *RARβ* were induced 1.5-fold to 3-fold (Fig. 6*B*). In liver, *CRBP1* levels were elevated two-fold; however, *CYP26A1* levels were dramatically decreased (Fig. 6*C*). We hypothesized that *CYP26A1* levels were decreased to compensate for the reduction in RA production, and thus we tested whether FEN could induce *CYP26A1* mRNA in this setting. *RALDH1* KO mice administered FEN and HF diet gained less body mass than mice fed HF diet (Fig. 6*D*). Strikingly, FEN-induced elevations in *CYP26A1* and *RARβ* in both WAT and liver (Fig. 6*E*). FEN lowers serum RBP4 protein

levels but also prevents obesity in *RBP4* KO mice (3). Thus, we tested whether similar gene expression alterations were present in *RBP4* KO mice. We found no significant changes in the expression of retinoid metabolism and signaling genes in liver or PG-WAT (Fig. 6*F*), strongly suggesting *RBP4* KO and FEN treatment have largely differing modes of action to improve insulin sensitivity.

DISCUSSION

Recent studies have identified important regulators of retinoid homeostasis as potential therapeutic targets for obesity (2,16–18). A major limitation to the use of retinol or retinyl-acetate has been the development of liver disease when these compounds are used in high doses for prolonged periods of time (27). However, FEN shows low toxicity compared with other retinoids (7,9,24). In this article, we show that FEN is a potent modulator of retinoid homeostasis genes in association with an improvement in whole-body physiology and in metabolically important genes.

CRBP1, *RARβ*, and *CYP26A1* are known RA-responsive genes because of the presence of RAREs located in their respective promoter regions. The upregulation of these proteins is thought to simultaneously promote the catabolism of RA and storage of retinol into retinyl-esters, thereby preventing the toxic effects of excess RA signaling mediated via RARs. These markers of RA signaling were found to be upregulated with long-term (20 weeks) or short-term (7 days) FEN treatment in all tissues examined (adipose, liver, and hypothalamus) and 3T3-L1 adipocytes. *CYP26A1* and *CRBP1* also were upregulated in cancer cells treated with FEN (28). Moreover, FEN-induced elevations in *CYP26A1* and *RARβ* independently of RALDH1 activity in HF-fed mice (Fig. 6*E*), indicating that increased RA production via RALDH1 is not required. Thus, it appears that FEN is directly or indirectly (or both) acting on RAREs in the promoters of these genes.

Many studies examining the effects of FEN on growth inhibition and apoptosis of cancer cell lines have concluded that FEN and RA exert their cellular effects through different pathways independent of *RAR* expression (29–31). For example, FEN and 4-MPR (the main catabolite of FEN) were found to bind poorly to recombinant RARs in vitro and only minimally activated RAREs and RXREs in cells (30). However, a role for the RARs has been supported by a number of other investigators. Fanjul et al. (32) demonstrated that 5–20 μmol/L FEN could transactivate *RARγ* and *RARβ*. *RARβ* expression is enhanced in normal human mammary cells after FEN exposure (33), and others have documented that *RARβ* or *RARγ* expression enhances FEN-mediated events (34,35). It is not clear why these contrasting results have been reported, but cell-type specific factors such as cofactor expression, epigenetic silencing, or phosphorylation may play a role (36–38).

Clearly, in 3T3-L1 cells, the differentiation process initiates a global downregulation of retinoid-responsive genes that FEN or RA is able to completely inhibit. It has been known that RA potently blocks adipogenesis when introduced at early stages of differentiation (13–15). Our results suggest that FEN acts similarly to RA in 3T3-L1 cells by blocking adipogenesis via inhibition of C/EBPβ-mediated transcription (39).

FEN modestly inhibited lipid accumulation in fully differentiated adipocytes (Fig. 2). These results are in marked
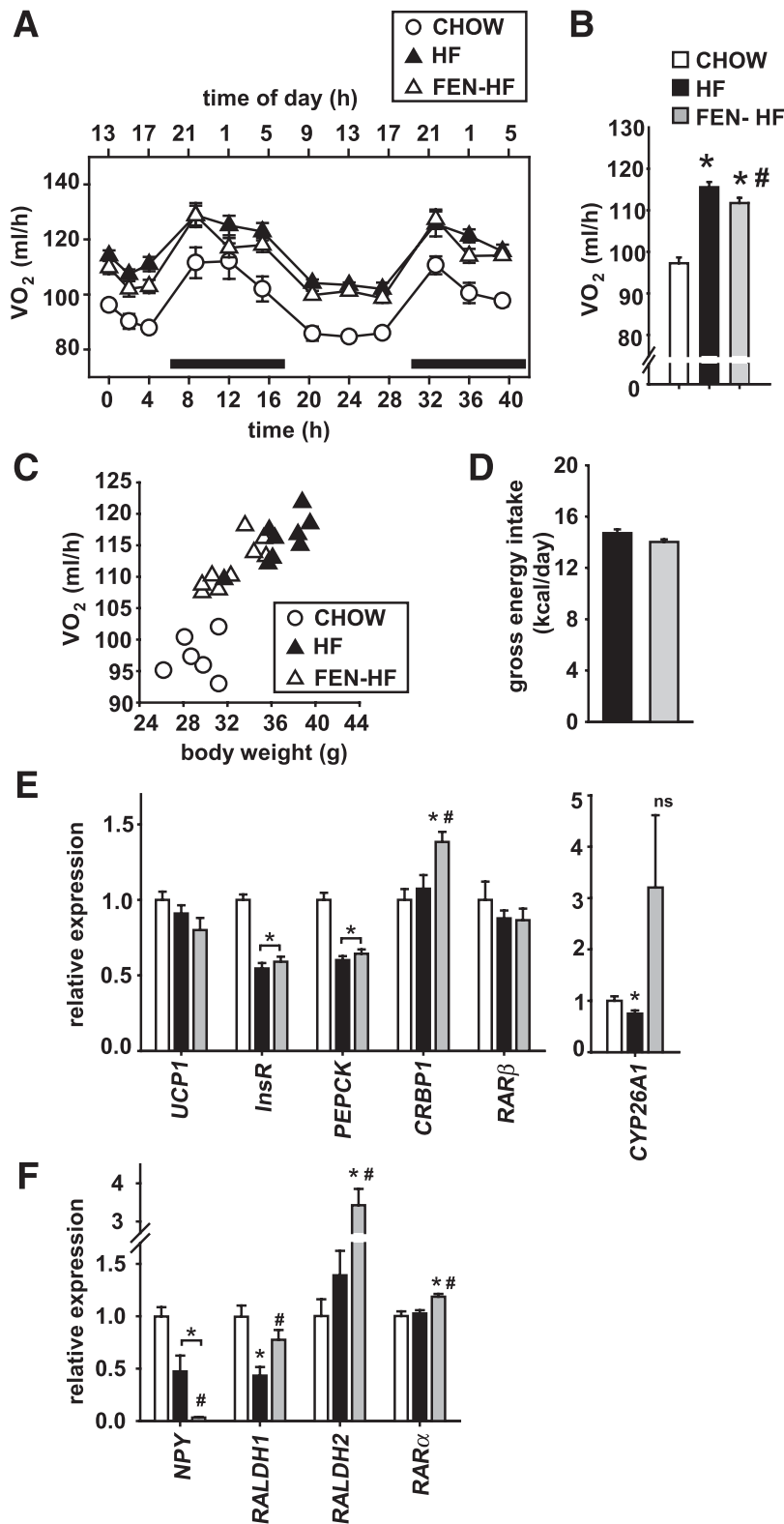
FIG. 4. FEN does not affect energy expenditure or brown adipose *UCP1* but completely suppresses hypothalamic *NPY*. *A–C*: Energy expenditure of mice during 4–6 weeks on diet during the night (indicated with black bar) and day (*A*), chow (clear circles), HF (black triangles), or FEN-HF (clear triangles), average over total time measured (*B*), (chow, clear bar; HF, black bar; or FEN-HF, gray bar), and positive correlation with body weight (*C*). $N = 6–9$ mice per dietary group. *$P < 0.05$ vs. chow by one-way ANOVA and Bonferroni post hoc test; #$P < 0.05$ by t test FEN-HF vs. HF. *D*: Gross energy intake during 12–30 days diet (up to energy expenditure measurement). FEN vs. HF is not significant. *E* and *F*: Relative gene expression levels in brown adipose tissue (*E*) and hypothalamus (*F*), chow (clear bars), HF (black bars), or FEN-HF (gray bars) from mice killed after 20 weeks on diets from 3 months of age. Molecular analysis was performed from 6–8 mice per dietary group. The t test was used to calculate significant difference for brown adipose tissue *CYP26A1* HF vs. chow for hypothalamic *RALDH1* and *RARα* FEN-HF vs. HF. Otherwise significance was calculated by ANOVA.
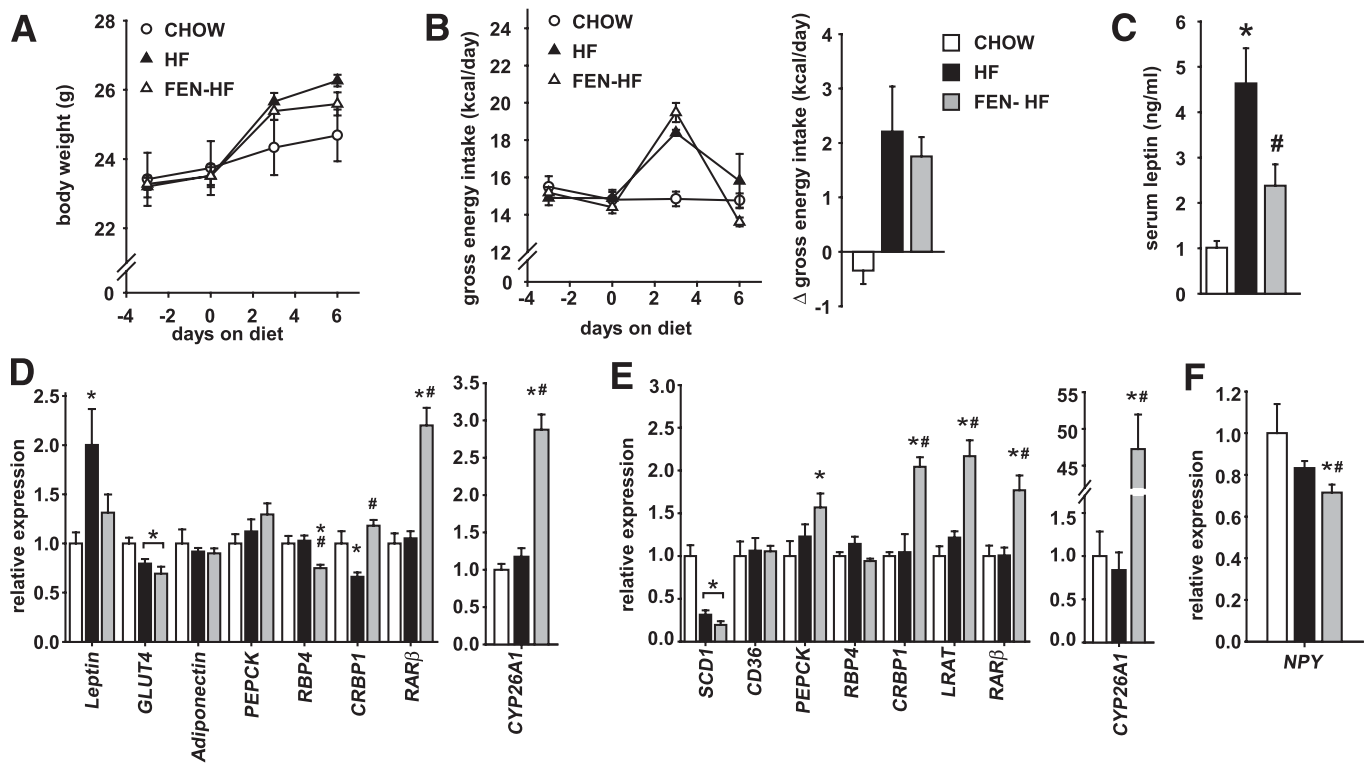
FIG. 5. Short-term FEN treatment inhibits HF induced hyperleptinemia and induces retinoid responsive genes. *A–C*: Male C57 BL/6 mice on chow (clear circles), HF (black triangles), or FEN-HF (clear triangles) for 1 week from 6 weeks age, $n = 8$ for each diet group. Body weight curves (*A*) and food intake (*B*) represented as gross energy intake (left panel) and change in intake from baseline (right panel) and serum leptin levels after 7 days diet (*C*). *D–F*: Relative gene expression levels in perigonadal adipose (*D*), liver (*E*), and hypothalami (*F*) after 7 days of diet, chow (clear bars), HF (black bars), or FEN-HF (gray bars). Molecular analysis was performed in 6–8 mice per dietary group. Significance indicated by *$P < 0.05$ vs. chow and #$P < 0.05$ vs. HF. The *t* test was used to calculate significant difference for perigonadal-WAT *GLUT4* HF vs. chow, liver *PEPCK* FEN vs. HF, and hypothalamic *NPY* FEN vs. HF. Otherwise significance was calculated by ANOVA.

contrast to those obtained with RA treatment (15), indicating that the exact mechanism of FEN action is not identical to that of RA. This may be because unlike RA, FEN leads to a global reduction in vitamin A levels because of the blockade of retinol transport and the renal loss of serum RBP4 in vivo. Short-term FEN treatment was sufficient to cause a downregulation in adipose *RBP4* both in C57Bl/6 mice and in *RALDH1* KO mice. Importantly, loss of *RBP4* alone was not sufficient to induce the gene expression changes seen with either FEN treatment or *RALDH1* genetic deletion. Thus, the effects of FEN are not simply attributable to its effects on RBP4 (3).

RA has been shown to inhibit leptin production or secretion (or both) in cells and in rodents (40,41). Paradoxically, RA also induces *UCP1* in brown adipose tissue to increase energy expenditure (42–44). FEN inhibited the HF-induced elevation in leptin serum levels and directly inhibited *leptin* mRNA by 75% in fully differentiated adipocytes. In a clinical trial in overweight women, FEN improved insulin sensitivity and decreased serum leptin levels (45). We did not detect a difference in food intake or an increase in energy expenditure or brown adipose tissue *UCP1* levels. However, we found that FEN completely suppressed hypothalamic *NPY* expression, and a similar decrease has been shown with a neuronal cell line treated with RA (46). This finding provides a specific mechanism for the complete suppression of hepatic glucose production seen during a euglycemic-hyperinsulinemic clamp (3) and complete normalization of HF-induced hyperglycemia seen in our studies and in those of Yang et al. (2),

because central administration of NPY can induce hepatic insulin resistance (47).

The importance of retinoid homeostasis in whole-body energy balance and glucose homeostasis has been highlighted in genetic KO studies (16–18). The *CRBP1* and *CRABP2* findings are consistent with our own because FEN-induced leanness is associated with robust upregulation of these genes in vivo and in 3T3-L1 adipocytes. In our studies, we confirmed that mice lacking *RALDH1* are resistant to HF-induced obesity; however, adipose *RALDH1* levels were decreased with long-term HF diet and FEN treatment partially prevented this decline. Moreover, embryonic fibroblasts from *RALDH1*-deficient mice are impaired in their ability to undergo adipogenesis compared with wild-type fibroblasts (16). Reduced PPARγ levels as the mechanism of impaired adipogenesis in *RALDH1* KO cells have been implicated (48). However, this phenotype is not consistent with that of the adipose PPARγ KO mice, which are insulin resistant and experience hepatic steatosis with an HF diet (49). We found adipose tissue of *RALDH1* KO mice fed an HF diet had higher levels of PPARγ, IR, GLUT4, and *adiponectin*, consistent with improved whole-body insulin sensitivity and glucose homeostasis. Moreover, inhibition of 3T3-L1 cell adipogenesis by RA or FEN is associated with a marked upregulation of *RALDH1*.

FEN is the most widely studied retinoid in clinical trials (10) and is currently undergoing phase II clinical trials for treatment of insulin resistance in obese humans with hepatic steatosis (6). There is an urgent need for efficient and
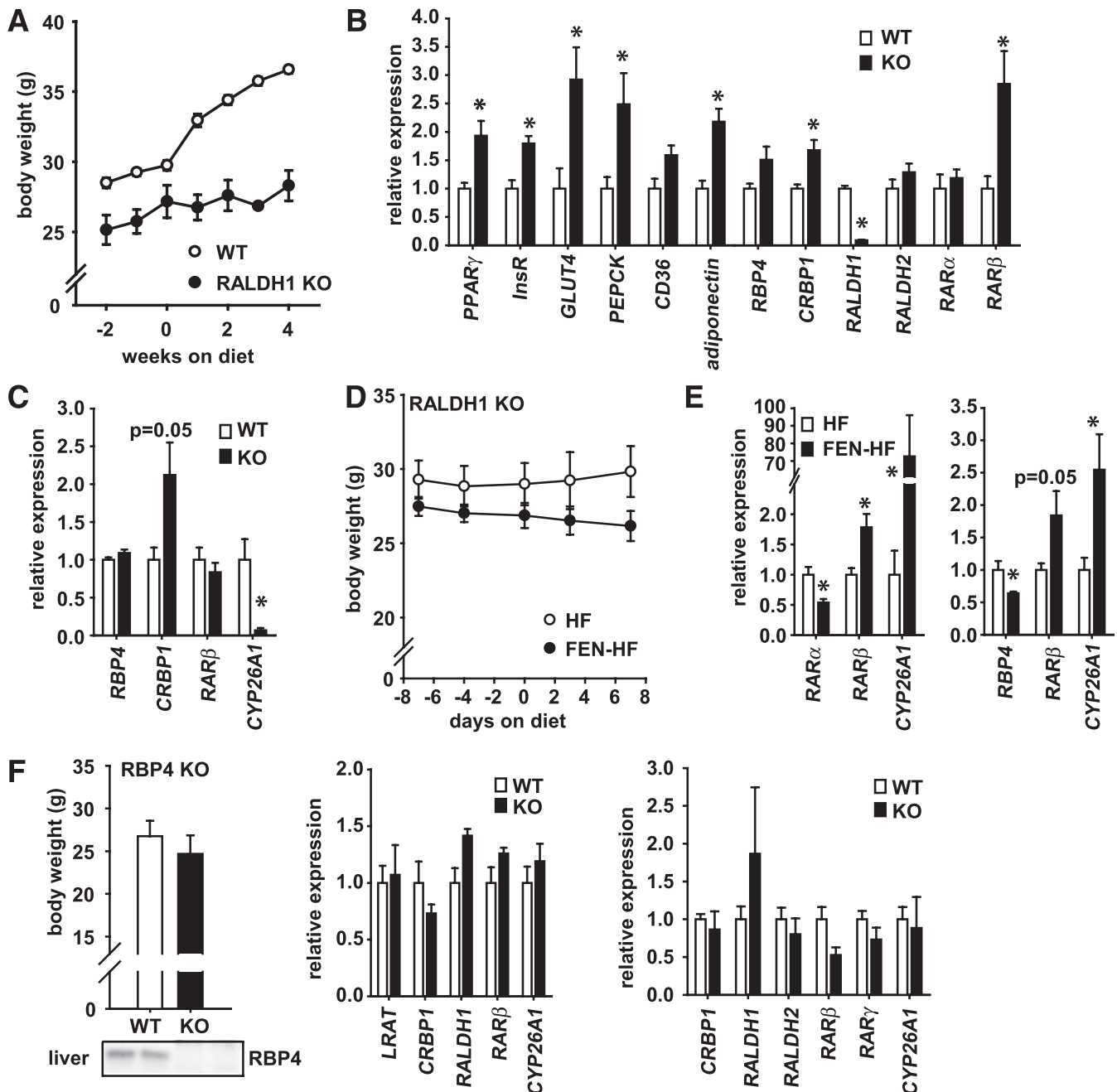
FIG. 6. FEN induces retinoid response genes in the absence of *RALDH1*. *A–C*: Male *RALDH1* KO (black circles) or wild-type (clear circles) mice on HF diet for 4 weeks, $n = 4$ for each diet group. Body weight curves (*A*) and relative gene expression levels in perigonadal adipose (*B*) and liver (*C*). *D* and *E*: Male *RALDH1* KO on HF (clear circles or bars) or FEN-HF (black circles or bars) for 1 week, $n = 5$ for each diet group. Body weight curves (*D*) and relative mRNA levels in liver and perigonadal adipose (*E*, left and right panels, respectively). *F*: Body weight of *RBP4* KO and wild-type controls and representative immunoblot of liver RBP4 protein levels (left panel). Relative gene expression levels in liver (middle panel) and perigonadal adipose (right panel). Significance (*$P < 0.05$) was calculated by *t* test.

nontoxic drugs to treat obesity and insulin resistance. FEN is relatively nontoxic and has been tested in phase III trials for cancer for periods of up to 5 years. Recently, a novel method to synthesize retinamides has produced a large library of *N*-(4-hydroxyphenyl)retinamide analogs (50). Although these retinamides have been evaluated for effects on tumor cells and cancer models, it might be useful to screen them for potentially superior effects on the metabolic syndrome. In line with recent studies that have shown that regulators of retinoid homeostasis are potential therapeutic targets for obesity, we present evidence that FEN also is a potent modulator of retinoid homeostasis genes in association with resistance to diet-induced obesity and insulin resistance.

REFERENCES

1. Nesto RW, Bell D, Bonow RO, et al. Thiazolidinedione use, fluid retention, and congestive heart failure: a consensus statement from the American Heart Association and American Diabetes Association.. Circulation 2003; 108:2941–2948
2. Yang Q, Graham TE, Mody N, et al. Serum retinol binding protein 4 contributes to insulin resistance in obesity and type 2 diabetes. Nature 2005; 436:356–362
3. Preitner F, Mody N, Graham TE, Peroni OD, Kahn BB. Long-term Fenretinide treatment prevents high-fat diet-induced obesity, insulin resistance, and hepatic steatosis. Am J Physiol Endocrinol Metab 2009;297: E1420–E1429
4. Berni R, Formelli F. In vitro interaction of fenretinide with plasma retinol-binding protein and its functional consequences. FEBS Lett 1992;308:43–45
5. Formelli F, Carsana R, Costa A, et al. Plasma retinol level reduction by the synthetic retinoid fenretinide: a one year follow-up study of breast cancer patients. Cancer Res 1989;49:6149–6152
6. Veterans Medical Research Foundation, University of California, San Diego. A randomized, double-blind study of the effects of fenretinide administered in subjects with obesity. ClinicalTrials.gov identifier: NCT00546455 2008
7. Moon RC, Thompson HJ, Becci PJ, et al. N-(4-Hydroxyphenyl)retinamide, a new retinoid for prevention of breast cancer in the rat. Cancer Res 1979; 39:1339–1346
8. Hail N Jr, Kim HJ, Lotan R. Mechanisms of fenretinide-induced apoptosis. Apoptosis 2006;11:1677–1694
9. Rotmensz N, De Palo G, Formelli F, et al. Long-term tolerability of fenretinide (4-HPR) in breast cancer patients. Eur J Cancer 1991;27:1127–1131
10. Zanardi S, Serrano D, Argusti A, Barile M, Puntoni M, Decensi A. Clinical trials with retinoids for breast cancer chemoprevention. Endocr Relat Cancer 2006;13:51–68
11. Decensi A, Torrisi R, Polizzi A, et al. Effect of the synthetic retinoid fenretinide on dark adaptation and the ocular surface. J Natl Cancer Inst 1994;86:105–110
12. Blomhoff R, Blomhoff HK. Overview of retinoid metabolism and function. J Neurobiol 2006;66:606–630
13. Sato M, Hiragun A, Mitsui H. Preadipocytes possess cellular retinoid binding proteins and their differentiation is inhibited by retinoids. Biochem Biophys Res Commun 1980;95:1839–1845
14. Murray T, Russell TR. Inhibition of adipose conversion in 3T3-L2 cells by retinoic acid. J Supramol Struct 1980;14:255–266
15. Xue JC, Schwarz EJ, Chawla A, Lazar MA. Distinct stages in adipogenesis revealed by retinoid inhibition of differentiation after induction of PPAR-gamma. Mol Cell Biol 1996;16:1567–1575
16. Ziouzenkova O, Orasanu G, Sharlach M, et al. Retinaldehyde represses adipogenesis and diet-induced obesity. Nat Med 2007;13:695–702
17. Zizola CF, Frey SK, Jitngarmkusol S, Kadereit B, Yan N, Vogel S. Cellular retinol-binding protein type I (CRBP-I) regulates adipogenesis. Mol Cell Biol 2010;30:3412–3420
18. Berry DC, DeSantis D, Soltanian H, Croniger CM, Noy N. Retinoic acid upregulates preadipocyte genes to block adipogenesis and suppress diet-induced obesity. Diabetes 2012;61:1112–1121
19. Molotkov A, Duester G. Genetic evidence that retinaldehyde dehydrogenase Raldh1 (Aldh1a1) functions downstream of alcohol dehydrogenase Adh1 in metabolism of retinol to retinoic acid. J Biol Chem 2003;278:36085–36090
20. Quadro L, Blaner WS, Salchow DJ, et al. Impaired retinal function and vitamin A availability in mice lacking retinol-binding protein. EMBO J 1999;18:4633–4644
21. Owen C, Czopek A, Agouni A, et al. Adipocyte-specific protein tyrosine phosphatase 1B deletion increases lipogenesis, adipocyte cell size and is a minor regulator of glucose homeostasis. PLoS ONE 2012;7: e32700
22. Pfaffl MW. A new mathematical model for relative quantification in real-time RT-PCR. Nucleic Acids Res 2001;29:e45
23. Mehta RG, Moon RC, Hawthorne M, Formelli F, Costa A. Distribution of fenretinide in the mammary gland of breast cancer patients. Eur J Cancer 1991;27:138–141
24. Formelli F, Clerici M, Campa T, et al. Five-year administration of fenretinide: pharmacokinetics and effects on plasma retinol concentrations. J Clin Oncol 1993;11:2036–2042
25. Flier JS. Insulin receptors and insulin resistance. Annu Rev Med 1983;34: 145–160
26. Tozzo E, Desbuquois B. Effects of STZ-induced diabetes and fasting on insulin receptor mRNA expression and insulin receptor gene transcription in rat liver. Diabetes 1992;41:1609–1616
27. Muenter MD, Perry HO, Ludwig J. Chronic vitamin A intoxication in adults. Hepatic, neurologic and dermatologic complications. Am J Med 1971;50: 129–136
28. Villani MG, Appierto V, Cavadini E, et al. Identification of the fenretinide metabolite 4-oxo-fenretinide present in human plasma and formed in human ovarian carcinoma cells through induction of cytochrome P450 26A1. Clin Cancer Res 2004;10:6265–6275
29. Delia D, Aiello A, Lombardi L, et al. N-(4-hydroxyphenyl)retinamide induces apoptosis of malignant hemopoietic cell lines including those unresponsive to retinoic acid. Cancer Res 1993;53:6036–6041
30. Sheikh MS, Shao ZM, Li XS, et al. N-(4-hydroxyphenyl)retinamide (4-HPR)-mediated biological actions involve retinoid receptor-independent pathways in human breast carcinoma. Carcinogenesis 1995;16:2477–2486
31. Fontana JA, Rishi AK. Classical and novel retinoids: their targets in cancer therapy. Leukemia 2002;16:463–472
32. Fanjul AN, Delia D, Pierotti MA, Rideout D, Yu JQ, Pfahl M. 4-Hydroxyphenyl retinamide is a highly selective activator of retinoid receptors [published correction appears in *J Biol Chem*. 1996;271(52):33705]. J Biol Chem 1996; 271:22441–22446
33. Swisshelm K, Ryan K, Lee X, Tsou HC, Peacocke M, Sager R. Down-regulation of retinoic acid receptor beta in mammary carcinoma cell lines and its up-regulation in senescing normal mammary epithelial cells. Cell Growth Differ 1994;5:133–141
34. Sabichi AL, Hendricks DT, Bober MA, Birrer MJ. Retinoic acid receptor beta expression and growth inhibition of gynecologic cancer cells by the synthetic retinoid N-(4-hydroxyphenyl) retinamide. J Natl Cancer Inst 1998;90:597–605
35. Liu G, Wu M, Levi G, Ferrari N. Inhibition of cancer cell growth by all-trans retinoic acid and its analog N-(4-hydroxyphenyl) retinamide: a possible mechanism of action via regulation of retinoid receptors expression. Int J Cancer 1998;78:248–254
36. Ren M, Pozzi S, Bistulfi G, Somenzi G, Rossetti S, Sacchi N. Impaired retinoic acid (RA) signal leads to RARbeta2 epigenetic silencing and RA resistance. Mol Cell Biol 2005;25:10591–10603
37. Bruck N, Vitoux D, Ferry C, et al. A coordinated phosphorylation cascade initiated by p38MAPK/MSK1 directs RARalpha to target promoters. EMBO J 2009;28:34–47
38. Wang A, Alimova IN, Luo P, Jong A, Triche TJ, Wu L. Loss of CAK phosphorylation of RARalpha mediates transcriptional control of retinoid-induced cancer cell differentiation. FASEB J 2010;24:833–843
39. Schwarz EJ, Reginato MJ, Shao D, Krakow SL, Lazar MA. Retinoic acid blocks adipogenesis by inhibiting C/EBPbeta-mediated transcription. Mol Cell Biol 1997;17:1552–1561
40. Kumar MV, Scarpace PJ. Differential effects of retinoic acid on uncoupling protein-1 and leptin gene expression. J Endocrinol 1998;157:237–243
41. Menendez C, Lage M, Peino R, et al. Retinoic acid and vitamin D(3) powerfully inhibit in vitro leptin secretion by human adipose tissue. J Endocrinol 2001;170:425–431
42. Alvarez R, de Andrés J, Yubero P, et al. A novel regulatory pathway of brown fat thermogenesis. Retinoic acid is a transcriptional activator of

the mitochondrial uncoupling protein gene. J Biol Chem 1995;270:5666–5673

43. Puigserver P, Vázquez F, Bonet ML, Picó C, Palou A. In vitro and in vivo induction of brown adipocyte uncoupling protein (thermogenin) by retinoic acid. Biochem J 1996;317:827–833

44. Kumar MV, Sunvold GD, Scarpace PJ. Dietary vitamin A supplementation in rats: suppression of leptin and induction of UCP1 mRNA. J Lipid Res 1999;40:824–829

45. Johansson H, Gandini S, Guerrieri-Gonzaga A, et al. Effect of fenretinide and low-dose tamoxifen on insulin sensitivity in premenopausal women at high risk for breast cancer. Cancer Res 2008;68:9512–9518

46. Magni P, Beretta E, Scaccianoce E, Motta M. Retinoic acid negatively regulates neuropeptide Y expression in human neuroblastoma cells. Neuropharmacology 2000;39:1628–1636

47. van den Hoek AM, van Heijningen C, Schröder-van der Elst JP, et al. Intracerebroventricular administration of neuropeptide Y induces hepatic insulin resistance via sympathetic innervation. Diabetes 2008;57:2304–2310

48. Reichert B, Yasmeen R, Jeyakumar SM, et al. Concerted action of aldehyde dehydrogenases influences depot-specific fat formation. Mol Endocrinol 2011;25:799–809

49. He W, Barak Y, Hevener A, et al. Adipose-specific peroxisome proliferator-activated receptor gamma knockout causes insulin resistance in fat and liver but not in muscle. Proc Natl Acad Sci USA 2003;100:15712–15717

50. Mershon SM, Anding AL, Chapman JS, Clagett-Dame M, Stonerock LA, Curley RW Jr. Solid phase-assisted synthesis and screening of a small library of N-(4-hydroxyphenyl)retinamide (4-HPR) analogs. Bioorg Med Chem Lett 2007;17:836–840